

Surface Assisted Nucleation and Growth of Polymer Latexes on Organically-Modified Inorganic Particles

Elodie Bourgeat-Lami,^{*1} Norma Negrete Herrera,¹ Jean-Luc Putaux,² Stéphane Reculusa,³ Adeline Perro,³ Serge Ravaine,³ Christophe Mingotaud,⁴ Etienne Duguet⁵

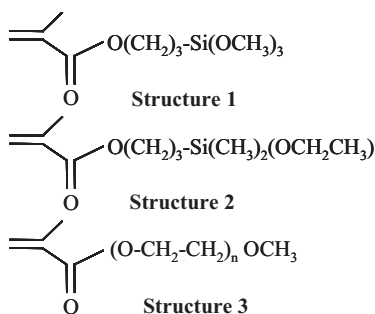
Summary: Polymer latex particles were synthesized in the presence of inorganic particles, which had been organically-modified to promote favorable interactions with growing macromolecules. The organic modification was performed using three different routes: (1) surface covalent grafting of vinyl trialkoxysilanes, (2) surface adsorption of polyethylene glycol-based macromonomers, and (3) bulk modification through ion exchange with cationic monomers or cationic initiators. Two types of mineral particles were studied: commercial and self-prepared silica particles (with diameters from 80 nm to 1 μm), and commercial laponite clay particles with a cation exchange capacity of 0.75 meq $\cdot \text{g}^{-1}$. Emulsion polymerization was performed in the presence of styrene or butyl acrylate monomers. The morphologies of the nanocomposite particles were observed by (cryogenic) transmission electron microscopy and correlated to the organic modification procedure.

Keywords: emulsion polymerization; laponite; nanocomposite colloids; organic modification; silicas

Introduction

The combination of organic polymers and inorganic colloids into nanocomposite particles has attracted considerable attention in recent years as these materials offer the prospect of new synergetic properties that originate from their organic and inorganic components.^[1–6] Organic/inorganic colloids can be produced by a variety of ways using either ex situ or in situ techniques. In situ techniques mostly involve polymerizing in the presence of mineral particles,

which have been functionalized in order to promote the formation of polymer on their surface.^[1] In the present paper, we report on the synthesis of polymer/silica and polymer/clay nanocomposite colloids through emulsion polymerization. Organic modification of the mineral particles is performed by grafting of organosilane molecules bearing a reactive methacrylate group (structures **1** and **2**),^[7–10] by adsorption of a methyl methacrylate-terminated polyethylene glycol macromonomer (structure **3**)^[11] or by ion exchange of a cationic monomer or a cationic initiator (structures **4** and **5**, respectively).^[12,13]



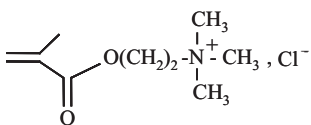
¹ Laboratoire de Chimie et Procédés de Polymérisation, CNRS-CPE Lyon, Bâtiment 308 F, 43, boulevard du 11 novembre 1918, BP 2077-69616 Villeurbanne Cedex, France

² Centre de Recherches sur les Macromolécules Végétales, ICMG/CNRS, BP 53, 38041 Grenoble Cedex 9, France

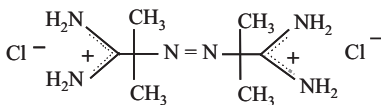
³ Centre de Recherche Paul Pascal, CNRS, 115, avenue du Dr Schweitzer, 33600 Pessac, France

⁴ Laboratoire des IMRCP—Université Paul Sabatier, 118, route de Narbonne, 31062 Toulouse Cedex, France

⁵ Institut de Chimie de la Matière Condensée de Bordeaux, CNRS-87, avenue du Dr Schweitzer, 33608 Pessac Cedex, France



Structure 4



Structure 5

The article is divided into two parts. In the first part, we describe the elaboration of silica/polystyrene composite particles following two procedures. The silica particles are indeed either functionalized by a trialkoxysilane carrying a polymerizable end group or surface-modified by adsorption of a polyethylene glycol-based macromonomer. The second part of the article is devoted to the synthesis of clay-based composite particles using organically-modified laponite particles as seeds. The clay particles were either grafted again by trialkoxysilane molecules or cation-exchanged with a bicationic initiator or a cationic monomer. The paper describes the surface modification of the mineral particles and addresses the effect of the experimental parameters on the composite particles morphology.

Experimental Part

Materials

The commercial silica sol with a diameter of 80 nm and a solid content of around 30% (Klebosol 30N50) was kindly supplied by Clariant and used as received. Suspensions of silica particles in a mixture of ethanol and water, with diameters of 500 nm and 1 μm , respectively, were prepared according to the procedure of Stöber et al. as described previously.^[11] They were evaporated in order to remove part of ammonia and ethanol and to reduce the volume of the suspension. The latter was then dialyzed against water until neutral pH. Its final concentration was determined gravimetrically and adjusted to the desired value before use. Laponite RD with a cation exchange capacity (CEC) of 0.75 meq $\cdot \text{g}^{-1}$

was supplied from Laporte Industries and used without further purification.

(γ -Methacryloyloxypropyl)trimethoxysilane (γ -MPS, $M_w = 248.3 \text{ g} \cdot \text{mol}^{-1}$, Aldrich), (γ -methacryloyloxypropyl)dimethylethoxysilane (γ -MPDES, $M_w = 230.3 \text{ g} \cdot \text{mol}^{-1}$, Gelest), 2,2-azobis(2-methylpropionamidine)hydrochloride (AIBA, $M_w = 271.2 \text{ g} \cdot \text{mol}^{-1}$, Acros Organics), and 2-(methacryloyloxyethyl)trimethyl ammonium chloride (MADQUAT, $M_w = 207.2 \text{ g} \cdot \text{mol}^{-1}$, a gift from ARKEMA) were used without further purification. The macromonomer, poly(ethylene glycol) 1000 monomethylether methacrylate (PEG methacrylate) was obtained from Polysciences. The peptizing agent, tetrasodium pyrophosphate ($\text{Na}_4\text{P}_2\text{O}_7$, Aldrich), the monomers, styrene (Aldrich) and butyl acrylate (Aldrich) and the initiators, potassium persulfate (KPS, Acros Organics) and azobis cyano pentanoic acid (ACPA, Wako Chemicals) were used as received. The anionic surfactant, sodium dodecyl sulfate (SDS, $M_w = 288.38 \text{ g} \cdot \text{mol}^{-1}$, Acros Organics) and the nonylphenol poly(oxyethylene) nonionic surfactant (Remcopal NP30, $M_w = 1540 \text{ g} \cdot \text{mol}^{-1}$, a gift from CECA S.A, Paris) were of analytical grade and used as supplied. Deionized water was purified by a Milli-Q Academic system (Millipore Cooperation).

Organic Modification Procedures

a) Silica

Grafting of the commercial Klebosol 30N50 silica sol was performed by introducing known amounts of MPS into 100 mL of a $10 \text{ g} \cdot \text{L}^{-1}$ stock silica suspension containing $1 \text{ g} \cdot \text{L}^{-1}$ of SDS. The dispersions were stirred magnetically at ambient temperature and allowed to equilibrate for 19 h. They were next centrifuged and the supernatant solutions were analyzed by UV spectroscopy. The amount of grafted MPS, Q_{MPS} ($\mu\text{mol} \cdot \text{m}^{-2}$), was determined by difference between the total amount and the free amount of MPS using a predetermined calibration curve established on silica-free suspensions of identical composition,

according to:

$$Q_{\text{MPS}} (\mu\text{mol} \cdot \text{m}^{-2}) = \frac{(C_0 - C_e)V}{M_w \times M \times S_{\text{spec}}} \times 10^6 \quad (1)$$

where C_0 ($\text{g} \cdot \text{L}^{-1}$) is the initial MPS concentration, C_e ($\text{g} \cdot \text{L}^{-1}$) is the MPS equilibrium concentration determined by UV analysis, V (l) designates the volume of solution, M (g) is the mass of silica, M_w ($\text{g} \cdot \text{mol}^{-1}$) is the molar mass of MPS, and S_{spec} ($\text{m}^2 \cdot \text{g}^{-1}$) is the specific surface area of silica.

S_{spec} was calculated using Equation (2) assuming that the particles are nonporous and spherical according to:

$$S_{\text{spec}} (\text{m}^2 \cdot \text{g}^{-1}) = \frac{6000}{\rho \times D_n} \quad (2)$$

where ρ ($\text{g} \cdot \text{cm}^{-3}$) is the density of silica and D_n (nm) is its number average particle diameter.

Macromonomer adsorption was performed by adding a known amount of a calibrated PEG methacrylate solution to a known amount of the aqueous silica suspension in a capped glass vessel. The dispersion was shaken magnetically at ambient temperature and allowed to equilibrate for 24 h. The macromonomer concentration was fixed to 1.5 μmol per square meter of silica.

b) Laponite

Grafting of the MPS and MPDES molecules on the laponite clay edges was performed as follows. 1 g of laponite was suspended into 100 mL of toluene and a known amount of the coupling agent (comprised between 0.75 and 7 mmol) was introduced in the reaction flask and allowed to react for 21 d at room temperature. The grafted laponites were filtered, extensively washed with toluene in order to remove the excess of functional alkoxysilane, and dried overnight in a vacuum oven at 40 °C before characterization.

The grafted amount (expressed in mmoles of grafted silane per gram of bare laponite) was determined from the differ-

ence ΔC (wt.-%) of carbon content after and before grafting as follows:

$$\begin{aligned} \text{Grafted amount (mmol} \cdot \text{g}^{-1}) \\ = \frac{10^3 \times \Delta C}{(1200 N_c - \Delta C(M - 1))} \end{aligned} \quad (3)$$

where N_c and M ($\text{g} \cdot \text{mol}^{-1}$) designate the number of carbon atoms and the molecular weight of the grafted silane molecule, respectively ($N_c = 7$ and $M = 206$ for MPS while $N_c = 9$ and $M = 202$ for MPDES).

The cation exchange was carried out as follows. 0.2 g of Na^+ -laponite was introduced into 70 mL of water and stirred until obtaining a transparent suspension. Then, a predetermined amount of AIBA or MADQUAT (respectively, 0.2 and 0.32 g) corresponding to approximately twice the CEC of laponite, was added to the clay suspension under magnetic stirring. The mixtures were stirred at room temperature for 3 h. The suspensions were then centrifuged at 5000 rpm and the amount of remaining cation was experimentally determined by UV titration from previously constructed calibration curves. The adsorbed amounts, Q_0 ($\text{mg} \cdot \text{g}^{-1}$), were calculated by difference between the total and the free concentrations according to:

$$Q_e = \frac{(C_0 - C_e)V}{M} \quad (4)$$

where C_0 ($\text{mg} \cdot \text{L}^{-1}$) is the initial AIBA or MADQUAT concentration, V (l) is the volume of solution, M (g) is the mass of laponite, and C_e ($\text{mg} \cdot \text{L}^{-1}$) designates the AIBA or MADQUAT equilibrium concentration determined either by UV analysis or from the carbon content (carbon, $\text{mg} \cdot \text{L}^{-1}$) of the supernatant solutions according to:

$$C_e = \frac{\text{Carbon}}{M_C \times N_C} \quad (5)$$

The precipitate was then extensively washed with water in order to remove the salt in excess, and dried at 40 °C in a vacuum oven for 24 h before characterization.

Emulsion Polymerization

Silica/Polystyrene Nanocomposite Particles

The polymerizations were carried out in batch at 70 °C for up to 24 h under nitrogen atmosphere. The 300 mL glass reactor fitted with a condenser was charged with the organically-modified silica suspension and the surfactant. Degassing was carried out for 30 min under gentle stirring before increasing the temperature up to 70 °C. Then, the initiator dissolved in 10 mL of de-ionized water and the monomer was added at once to start polymerization. Typical recipes are as follows: silica, 1 g; water, 100 g; styrene, 10 g; KPS, 0.1 g; and various amounts of surfactants.

Clay/poly(styrene-co-butyl acrylate) (poly(sty-BA) Nanocomposite Particles

Emulsion polymerization was carried out at 70 °C in a 250 mL three-necked double wall reactor equipped with a condenser, a nitrogen inlet tube, and a stirrer. A typical recipe for the grafted laponites is as follows. The reactor was charged with 100 g of the aqueous MPDES-grafted laponite suspensions ($10 \text{ g} \cdot \text{L}^{-1}$) containing the surfactant (SDS, $2 \text{ g} \cdot \text{L}^{-1}$) and the peptizing agent ($\text{Na}_4\text{P}_2\text{O}_7$, $1 \text{ g} \cdot \text{L}^{-1}$). After degassing, the monomers, a mixture of styrene (3 g) and butyl acrylate (7 g), and the initiator (ACPA, 0.1 g) were successively introduced at 70 °C under stirring.

Polymerizations performed using cation-exchanged clay particles involved slightly different experimental conditions. In a typical procedure, the AIBA-laponite or MADQUAT-laponite intercalation complexes were redispersed in water by introducing 1 g of the pyrophosphate agent per liter of suspension, sonicated for 3 min (Branson Unifier, 95% output power), and magnetically stirred for 2 h. Then, the required amount of surfactant and monomer was introduced in the clay suspension and the mixture was sonicated for 2 min (Branson Unifier, 95% output power). This procedure will be referred to as a “mini-emulsion-like” polymerization as it is similar to miniemulsion except that no

hydrophobe was used to stabilize the droplets. The polymerization was initiated by increasing the temperature in the case of the AIBA-laponite intercalation complex and by introducing 0.05 g of ACPA dissolved into 3 mL of water in the case of MADQUAT-laponite.

Characterizations

^{29}Si solid-state nuclear magnetic resonance (NMR) was performed on a Bruker DSX-300 spectrometer operating at 59.63 MHz, by use of cross-polarization from proton. The contact time was 5 ms, the recycle delay 1 s and the spinning rate 10 kHz. A JEOL JCSA 733 electron microprobe analyzer (EPMA) was used to determine the carbon content of the bare and organically-modified silicas. UV analysis was performed using an UV/VIS spectrophotometer and quartz cells. The measurements were carried out at the wavelength of 193 nm for AIBA and at 210 nm for MADQUAT. The X-ray diffraction (XRD) patterns were obtained from a Siemens D500 X-ray powder diffractometer (Ni-filtered $\text{CuK}\alpha$ rad, $\lambda = 1.5405 \text{ \AA}$). The d_{001} basal spacings were calculated from the 2θ values using the EVA software.

The monomer-to-polymer conversions were determined gravimetrically. Typically, 3–7 g of the latex suspension was placed in an aluminum dish and dried to constant weight at 70 °C. The morphology of the nanocomposite particles was characterized by “conventional” transmission electron microscopy (TEM) and cryogenic transmission electron microscopy (cryo-TEM). Specimens for TEM were prepared by evaporating one drop of dilute latex ($10^{-3}/10^{-6} \text{ g} \cdot \text{cm}^{-3}$) on a 200 mesh formvar-coated copper electron microscope grid. The grids were placed in the vacuum chamber of a Philips CM120 electron microscope operating at 80 kV and observed under low illumination dose. The diameters of the polymer particles were measured directly from the electron micrographs. A minimum of 100 particles was counted for each batch. The number of average diameter, D_n , was calculated using

Equation (4) where n_i designates the number of particles of diameter D_i .

$$D_n = \frac{\sum n_i D_i}{\sum n_i} \quad (6)$$

The weight average diameter, D_w , was calculated from:

$$D_w = \frac{\sum n_i D_i^4}{\sum n_i D_i^3} \quad (7)$$

and the polydispersity index (PDI) was given by:

$$\text{PDI} = \frac{D_w}{D_n} \quad (8)$$

Following procedures described elsewhere,^[14–16] specimens for cryo-TEM analysis were prepared by quench-freezing thin films of the latex suspensions in liquid ethane. They were then mounted in a Gatan 626 cryo-holder, transferred in a Philips CM200 “Cryo” electron microscope operating at 80 kV, and observed at low temperature (−180 °C) under low dose illumination. Images were recorded on Kodak SO163 films.

The particle number per unit volume of water (N_p/L) was calculated by the following equation:

$$N_p/L = \frac{\frac{M}{\rho}}{\frac{\pi}{6} D_n^3 \cdot V} \times 10^{19} \quad (9)$$

where M (g) is the total mass of solid, ρ (g · cm^{−3}) is the density of the particles, D_n (nm) is the number average particles diameter determined either from the TEM micrographs or by DLS, and V (in liter) is the total volume of water.

Results and Discussion

Silica/Polystyrene Composite Particles

Grafting of (γ -methacryloyloxypropyl)-trimethoxysilane

The grafting was carried out at pH = 9.5 by adding MPS to the aqueous colloidal suspension of the Klebosol 30N50 silica particles containing 1 g · L^{−1} of the anionic SDS surfactant. The role of the surfactant is

to help disperse the MPS molecules in water and also to reduce the size of the polycondensates that might be formed in the surrounding aqueous solution. Indeed, the functional trialkoxysilane molecules may either undergo (i) reaction with the silanol groups of silica or (ii) form a polysilsesquioxane (PSSO) network through hydrolysis and self-condensation in the surrounding solution. The PSSO network can in turn graft to the surface forming a polysiloxane coating or stabilize in the water suspension forming somehow new particles or clusters. The amount of chemisorbed MPS was determined by UV analysis titration of the supernatant solutions recovered by centrifugation of the suspension medium according to the so-called depletion method. This method allows accurate determination of the MPS grafting density even for low initial concentrations. However, in order to quantitatively determine the amount of residual trialkoxysilane in the water solution after removal of the grafted silica particles, reaction following Scheme 2 should not yield too large particles as these particles would not be separated from silica. This was ensured by the addition of surfactant in the water phase that allowed to stabilize the polycondensates and significantly reduce their size.

Figure 1 shows the evolution of the MPS grafting density as a function of the initial MPS concentration. The grafting density increases with increasing the silane content and reaches a plateau at high concentrations. It is worthwhile to notice that a similar behavior has been reported in the literature for related systems.^[17]

Controlling the MPS grafting density is essential as the double bonds are expected to react with the growing polystyryl radicals, and thus promote anchoring of the polystyrene chains on silica. In order to investigate the effect of the amount of double bonds on the composite particles morphology, a series of polymerization experiments were performed in the presence of the MPS-grafted silica suspensions with increasing grafting densities. All the

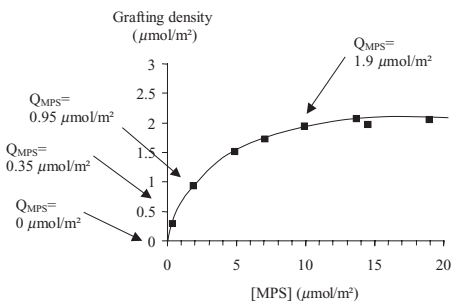


Figure 1.

MPS grafting density as a function of the initial MPS concentration. The grafting was performed by direct addition of MPS to a $10 \text{ g} \cdot \text{L}^{-1}$ aqueous Klebosol 30N50 silica particles suspension containing $1 \text{ g} \cdot \text{L}^{-1}$ SDS. The reaction was carried out at $\text{pH} = 9.3$ for 19 h under magnetic stirring.

polymerizations were performed under otherwise identical conditions in order to analyze the effect of the MPS grafting density only. The conditions for this series of experiments are the following: $[\text{MPS-functionalized silica}] = 10 \text{ g} \cdot \text{L}^{-1}$, $[\text{SDS}] = 1 \text{ g} \cdot \text{L}^{-1}$, $[\text{styrene}] = 100 \text{ g} \cdot \text{L}^{-1}$, and $[\text{KPS}] = 0.5 \text{ g} \cdot \text{L}^{-1}$. Figure 2 shows the TEM images obtained for grafting densities of 0, 0.95 and $1.9 \text{ } \mu\text{mol} \cdot \text{m}^{-2}$, respectively (see the arrows in Figure 1). For the sake of clarity, micrographs were recorded at low

and high magnification to better visualize the particles shape. It can be seen from Figure 2 that only the polymerization performed in the presence of nongrafted silica particles gave rise to separate populations of silica beads and polymer latexes with no apparent interactions between them. For all the other experiments, the latex spheres showed more or less affinity for the silica surface indicating that the organic modification is essential in order to yield nanocomposite particle morphologies.

For very low MPS grafting densities (typically below $0.5 \text{ } \mu\text{mol} \cdot \text{m}^{-2}$), irregular daisy-shaped morphologies were produced with only a few colloids surrounding the silica spheres in an irregular fashion.^[8] When the MPS grafting density increases and reaches a value close to, e.g., $1 \text{ } \mu\text{mol} \cdot \text{m}^{-2}$, most of the polymer latexes are located around the silica particles in more regular flower-like morphologies, each particle being surrounded in average by eight polystyrene petals, as determined by the ratio of the number of polymer particles to the number of silica particles. With increasing further the MPS grafting density, core-shell particles were obtained as shown in Figure 2c. What is also noticeable on

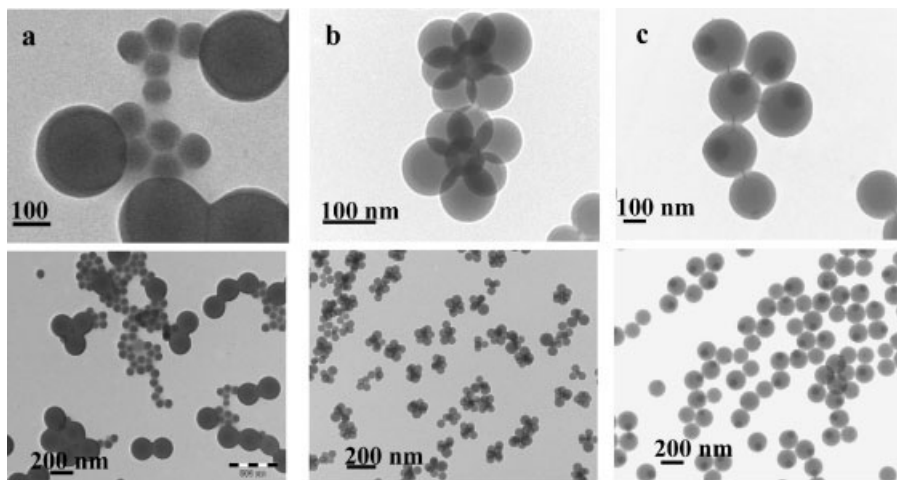


Figure 2.

TEM images of Klebosol 30N50 silica/polystyrene composite particles obtained for different MPS grafting densities. (a) Without MPS, (b) $Q_{\text{MPS}} = 0.95 \text{ } \mu\text{mol} \cdot \text{m}^{-2}$, and (c) $Q_{\text{MPS}} = 1.9 \text{ } \mu\text{mol} \cdot \text{m}^{-2}$. The images were recorded at low (bottom) and high magnifications (top).

Table 1.

Number average particle diameters, weight average particle diameters, and PDIs of polystyrene latex particles synthesized in the presence of MPS-grafted 30N50 silica particles with increasing MPS grafting densities.

MPS	Q_{MPS}	Conversion	D_n	D_w	$\frac{D_w}{D_n}$
$\mu\text{mol} \cdot \text{m}^{-2}$	$\mu\text{mol} \cdot \text{m}^{-2}$	%			
0	0	100	197.2	201.1	1.02
0.1	0.1	96	129.5	143.4	1.11
0.2	0.2	95	113.9	128.3	1.13
0.5	0.35	86	92.8	113.6	1.22
1	0.65	96.2	110.5	122.6	1.11
2	0.95	99.6	113.0	116.9	1.03
10	1.9	98.5	190.5	194.3	1.02

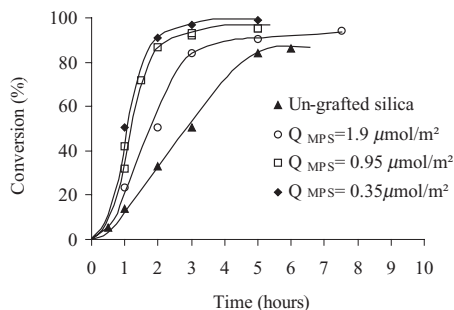
$[\text{SiO}_2] = 10 \text{ g} \cdot \text{L}^{-1}$, $[\text{SDS}] = 1 \text{ g} \cdot \text{L}^{-1}$, $[\text{styrene}] = 100 \text{ g} \cdot \text{L}^{-1}$, $[\text{KPS}] = 0.5 \text{ wt.-%}$ relative to styrene.

these TEM pictures is that the diameter of the polystyrene particles is not constant in the different experiments, and so is therefore the overall particle number and overall surface area.

Table 1 summarizes the particle size and size distribution of the polystyrene latexes directly determined from the TEM micrographs as a function of the MPS grafting density.

It can be seen that the diameter of the polystyrene latex particles decreases with increasing the MPS grafting density and then increases for larger MPS concentrations to reach a value which is close to that measured in the absence of silica particles. This result suggests that for low MPS grafting densities, the silica particles are able to stabilize the growing polymer spheres and generate a greater latex particle number than when SDS is used as surfactant alone. This is presumably due to the presence of negative charges on the silica surface that enables electrostatic stabilization of the growing polystyrene nodules. However, when the MPS grafting density increases, the polymer spheres no longer phase-segregate on the silica surface and the diameter of the resulting core-shell composite particles increases to reach the value corresponding to pure polymer particles stabilized by surfactant only.

As it is known that the rate of an emulsion polymerization is proportional to

**Figure 3.**

Conversion versus time curves for polymerization of styrene performed in the presence of Klebosol 30N50 silica particles with increasing amounts of MPS on their surface. Q_{MPS} indicates the actual MPS grafting density as determined by UV analysis using the depletion method.

the particle number, changes in particles size are also accompanied by strong variations in polymerization kinetics as shown in Figure 3. The lower the particles size, the higher the polymerization rate.

The mechanism of formation of the silica/polystyrene composite particles using MPS as coupling agent can be explained as follows. First, persulfate initiator starts to decompose in the water phase giving rise to the formation of radicals. These radicals will propagate with aqueous phase monomers until they undergo one of the following fates: (i) aqueous phase termination or (ii) entry into a micelle or precipitation (depending on the surfactant concentration), creating somehow a new particle. Aqueous-phase oligomers of all degrees of polymerization can also undergo frequent collision with the surface of the silica seed particles, and have therefore a high probability to copolymerize with the double bonds at the silica surface, thus generating chemisorbed polymer chains in the early stages of polymerization.

These discrete loci of adsorption are preferred to adsorb further oligomers or radicals compared with the bare seed surface. As a result, these discrete loci of adsorption become discrete loci of polymerization. The higher the MPS grafting density, the higher the probability of radical

capture by silica and therefore the higher the affinity of the growing polymer for the surface. The nucleated polystyrene nodules can thus coalesce and form a homogeneous coating around the silica seed particles; whereas for low MPS grafting densities, the hydrophilic nature of the surface promotes phase segregation of the growing polymer spheres.

Adsorption of a Polyethylene Glycol-Based Macromonomer

Apart from the use of functional alkoxy-silane molecules, silica/polystyrene composite particles with a raspberry-like morphology have been elaborated in the presence of a methyl methacrylate-terminated polyethylene glycol macromonomer. This macromonomer is mainly hydrophilic due to the presence of ethylene oxide groups ($n \sim 23$), which are able to form hydrogen bonds with silanol functions present on the silica surface. It is indeed well-known that poly(ethylene oxide) strongly adsorbs onto silica nanospheres.^[18]

At one of its ends, this molecule also contains a methacrylate group that constitutes a polymerizable group for the later reaction of styrene. This method involves three distinct stages. First, monodisperse silica particles with diameters in the micron size range are produced according to procedures inspired from the literature.^[19,20] The second step involves the adsorption of the macromonomer, as described in the “Experimental Part.” Finally, synthesis of the polystyrene particles is achieved through emulsion polymerization of styrene by heating the system in presence of a nonionic surfactant (Remco-pal NP30) and an initiator (sodium persulfate). Once the reaction is completed, hybrid particles with a raspberry-like morphology are obtained. All the experiments were performed with a macromonomer concentration of 1.5 μmol per square meter of silica and a constant silica concentration (typically 10 $\text{g} \cdot \text{L}^{-1}$), irrespective of the diameter of the silica particles.

Figure 4 shows the TEM micrograph of the resulting composite particles obtained

for different silica particles size while the mechanism involved in the formation of the nanohybrids is schematically represented in Scheme 1.

During the very first stages of the reaction, all the polymer nodules that are formed are adsorbed onto the mineral silica surface. This observation has already been confirmed by TEM experiments indicating that no free polymer particles are present in the bulk. However, when time is increasing, the diameter of the polymer particles becomes larger and larger until there is no more free and available space for them to stay adsorbed onto the inorganic surface. In other words, only a few polymer nodules can grow until reaching their final size without leaving the silica surface, some of the initially “weakly-adsorbed” nodules being expelled from the particle surface due to the growth of their “strongly-adsorbed” neighbors. This critical number can roughly be estimated while calculating the ratio between the whole surface of a single silica particle and the (projected) surface occupied by a polymer nodule, which is a function of time, and assuming that the nodules are more or less closely packed like in a hexagonal lattice. Indeed, SEM experiments have clearly shown that the polymer nodules were closely packed onto the silica surface at any time, and that their number decreases with time; whereas TEM pictures of a bulk sample extracted at different times indicate that the number of free polymer nodules, i.e., nodules not adsorbed onto silica, increases with time. Due to the large difference between silica and polystyrene densities, it is however possible and very easy to separate by centrifugation the organic-inorganic hybrid colloids from the free polymer nodules and observe the morphology of the hybrid particles alone, as it can be seen in Figure 5, whatever the reaction time.

Given the complex nature of our reaction medium—remembering that apart from the silica dialysis, we get raspberry-like particles in a one-pot synthesis—it is quite difficult to explain the observed phenomenon with accuracy. However, we can briefly describe our system as a

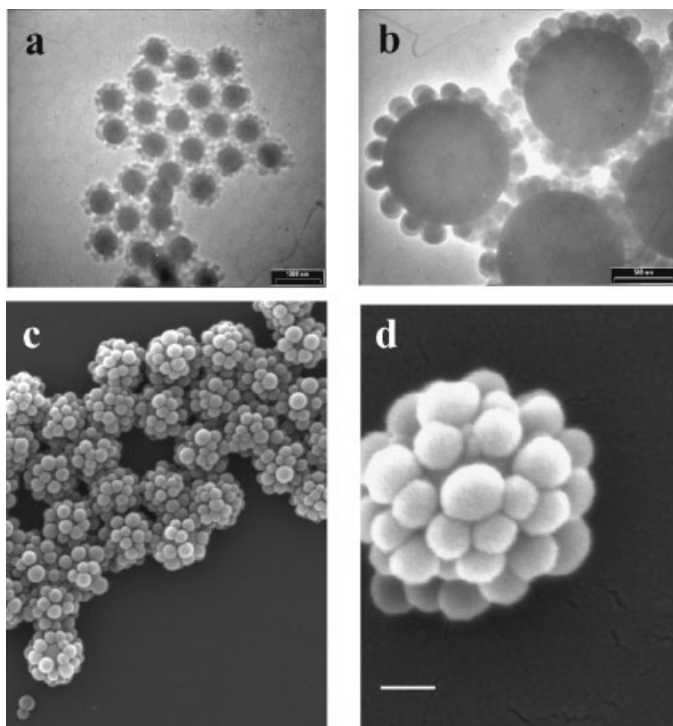


Figure 4.

TEM (a, b) and SEM (c, d) images of raspberry-like hybrids based on 500 nm (left) and 1 μm (right) Stöber silica particles. Scale bar: 500 nm.

self-stabilized copolymerization between the PEG macromonomer and styrene.

During the early steps of polymerization, free molecules of monomer and PEG methacrylate react to form copolymers. These copolymers will continue to grow

until they reach a critical size and become nuclei. Due to the presence of ethylene oxide groups in the structure of the macromonomer, and also because of the presence of the surfactant, these nuclei can become steady and evolve as mature



Scheme 1.

Schematic representation of the process involved in the synthesis of the silica/polystyrene raspberry-like composite particles.

polymer particles.^[21] This scenario also holds for the macromonomer adsorbed on the silica surface. In that case, the growing copolymers are expected to strongly attach on silica via the anchored PEG derivative. Free PEG molecules are also initially present in the suspension medium but it can be anticipated that the particles, or at least the copolymers they form with styrene, will also have a strong tendency to adsorb on silica.

Laponite/poly(sty-BA) Composite Particles

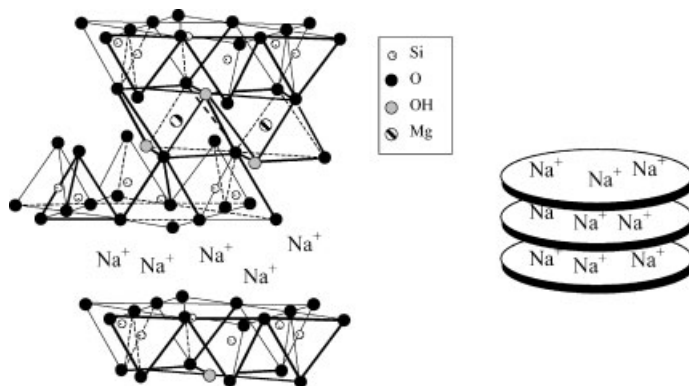
Clay Structure

Laponite RD is a fully synthetic clay similar in structure and composition to natural hectorite of the smectite group (Scheme 2). Each layer is composed of three sheets: two outer tetrahedral silica sheets and a central octahedral magnesia sheet. Isomorphous substitution of magnesium with lithium in the central sheet creates a net negative charge compensated by intralayer sodium ions located between adjacent layers in a stack. The CEC of laponite is 0.75 meq·g⁻¹.^[22] The dimensions of the elementary platelets are the following: diameter 30 nm and thickness 0.9 nm. In the dry state or in organic solvents, the platelets are piled up into tactoids of around 2–3 layers thick held together by long-range attractive forces. Reactive silanols, corresponding to structural defects, are located at the broken

edges of these stacks while MgOH groups are contained into the internal space of the individual clay sheets.

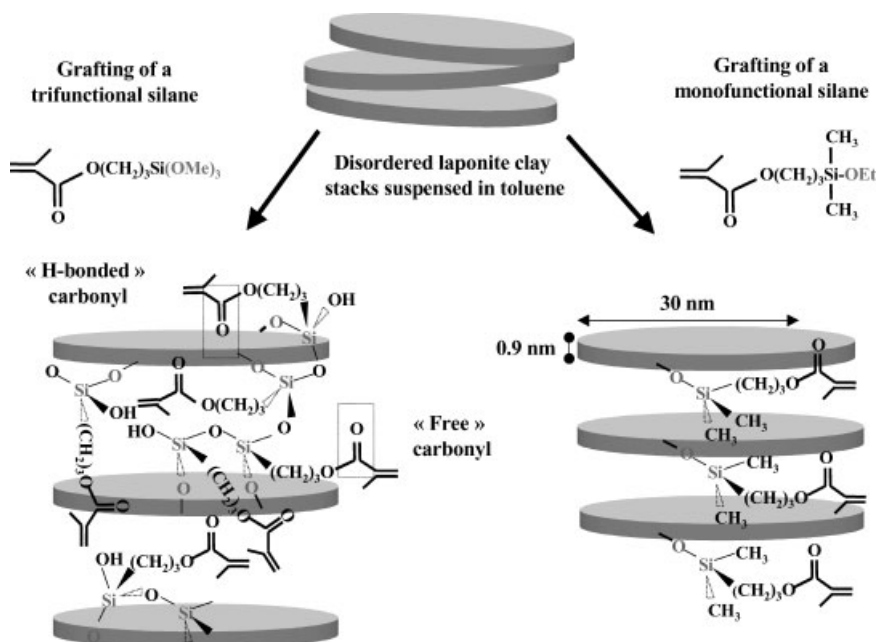
Grafting of the MPS and MPDES Molecules

Grafting of the functional alkoxyxilanes was performed in toluene by adding increasing amounts of the coupling agents to the clay suspension. The grafting was qualitatively evidenced by FTIR, ²⁹Si and ¹³C solid state NMR while the grafted amount was determined by carbon elemental analysis. FTIR indicates successful reaction of the organosilane molecules with the clay edges ($\nu_{\text{C=O}}$, 1700 cm⁻¹; ν_{CH} , 2850, 2920, and 2980 cm⁻¹ and δ_{CH} , 1380 cm⁻¹). More in-depth examination of the carbonyl region showed that both the MPS and the MPDES coupling agents formed hydrogen bonds with the clay surface as the signal of the carbonyl group, which can be detected at 1720 cm⁻¹ in the original grafted molecules, was shifted to a lower wave number. However, in case of the trialkoxyxilane MPS coupling agent, a shoulder at 1720 cm⁻¹, which can be assigned to free carbonyl groups, appeared for high grafting densities suggesting the formation of a multilayer coverage. Indeed, MPS molecules can undergo self-condensation in the presence of water giving rise to the formation of polysiloxane oligomers that are attached to the clay edges. These oligomers can also link together the



Scheme 2.

Laponite clay structure.



Scheme 3.

Schematic representation of the grafting reaction of organosilane molecules on laponite clay particles.

individual platelets and neighboring clay stacks as illustrated in Scheme 3. Contrary to the trialkoxysilane, the MPDES coupling agent cannot condense in solution and forms a monolayer coverage lying flat on the border of the clay plates.

Synthesis of the nanocomposite latexes in the presence of grafted laponite was carried out using 1 g of the organically-modified laponite suspended into 100 g of water in the presence of SDS and of the peptizing agent in order to facilitate clay redispersion in water. Under such conditions, satisfactory clay suspensions were obtained in case of the MPDES-grafted laponite whereas we did not succeed in redispersing the MPS-grafted clay. We presume that this is due to the fact that the clay platelets are irreversibly locked together by siloxane bridges bonding the clay edges as mentioned above. Therefore, in the following, only clay particles modified with the MPDES coupling agent will be involved in the polymerization reaction.

Figure 5b shows a cryogenic TEM micrograph of ca. 120 nm copolymer/laponite nanocomposite particles obtained

using MPDES-grafted laponite as the seed while the micrograph of Figure 5a corresponds to a sample prepared by emulsion polymerization in the presence of raw laponite. As mentioned in a previous work,^[10] laponite crystals appear as dark “filaments” and polymer particles as gray spheres. As expected, no particular interaction could be detected in Figure 5a between the clay platelets and the latex particles. Moreover, clay aggregates can be clearly seen in between the latex spheres. In contrast, when the monofunctional silane molecule was used as coupling agent, the clay platelets were homogeneously distributed within the latex sample and formed a nanocomposite structure, the clay constituting somehow the “shell” of the composite latexes. Moreover, it is worthwhile noticing that the particles are slightly polygonal as the natural rigidity of laponite crystals generates a faceting of the surface.

It must be underlined that noticeable differences in colloidal stability were observed when bare laponite was introduced in the polymerization reaction. Although the latexes were stable just after

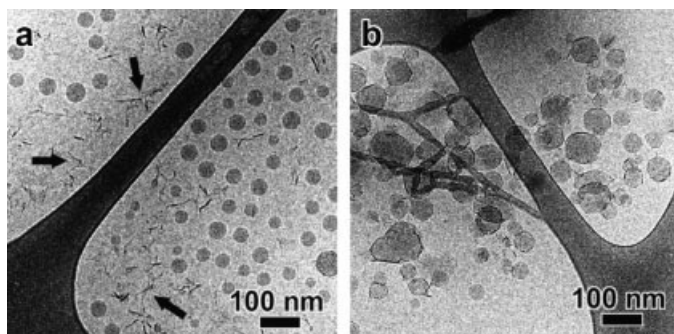


Figure 5.

Cryo-TEM images of (a) “hybrid latexes” synthesized by seeded emulsion polymerization of styrene and butyl acrylate in the presence of raw laponite (laponite aggregation is indicated by arrows) and (b) 10 wt.-% of MPDES-functionalized laponite clay platelets.

polymerization, they showed only a limited stability with time and coagulation was systematically observed upon storage. This is presumably related to the fact that as the clay platelets were not incorporated within the latex particles, they could form a gel in a similar way as they do in pure water solutions, a mechanism which is additionally promoted by the high ionic strength of the suspension medium. In contrast, successful incorporation of the clay sheets within the polymer particles allowed to achieve a better long-term stability of the suspension medium as there were no “free” clay platelets present in the surrounding aqueous solution.

Incorporation of Reactive Functional Groups Through Cation Exchange

Since laponite contains exchangeable sodium counter ions saturating the structural negative charges of the clay, organic cations can be introduced on its surface through cation exchange. Source of negative charges in laponite are both from isomorphic substitution (permanent charges) and broken edges (pH dependent). Isomorphic substitution is due to substitution within the lattice structure of lithium ions by magnesium ions. The edges are pH dependent due to the presence of amphoteric groups: MgOH, LiOH, and SiOH. These surface groups can be protonated or deprotonated depending on the

pH value of the surrounding solution. While MgOH and LiOH are positively charged below pH=9, SiOH groups are negatively charged.^[23,24] It should be noticed that the edge charge represents less than 10% of the total CEC of the mineral.^[25]

Qualitative evidence of the presence of either AIBA or MADQUAT in the inter-layer space of laponite was again provided by FTIR and solid state NMR spectroscopy (spectra not shown).^[12,13] Apart from qualitative investigations, we were also interested in quantitative determination of the amount of intercalated cations. The addition of either AIBA or MADQUAT to the aqueous laponite suspension, well above the CEC, resulted in clay flocculation which enabled easy determination of the residual cation concentration in the upper limpid supernatant solution by UV and carbon elemental analysis. Additional centrifugation of the clay suspension was performed in order to ensure that the supernatant solutions were free from any residual exfoliated clay sheets that could not be seen to the naked eye. The organic cation concentration on the clay surface was then determined by difference between the total amount and the free amount of cation. The amounts of cationic monomer incorporated within the clay structure for are indicated in Table 2.

As one AIBA molecules can potentially exchange two sodium counter-ions, the

Table 2.

Initial AIBA and MADQUAT concentrations and adsorbed amounts determined by UV and carbon elemental analysis of the supernatant solutions using the depletion method.

Samples	AIBA-laponite	MADQUAT-laponite
Initial concentrations ($\text{mmol} \cdot \text{L}^{-1}$)	7.4	15.4
Adsorbed amounts ($\text{mmol} \cdot \text{g}^{-1}$)		
UV ^a	0.37	0.65
EA ^b	0.36	0.63

^a Determined by UV analysis of the supernatant solutions using Equation (4).

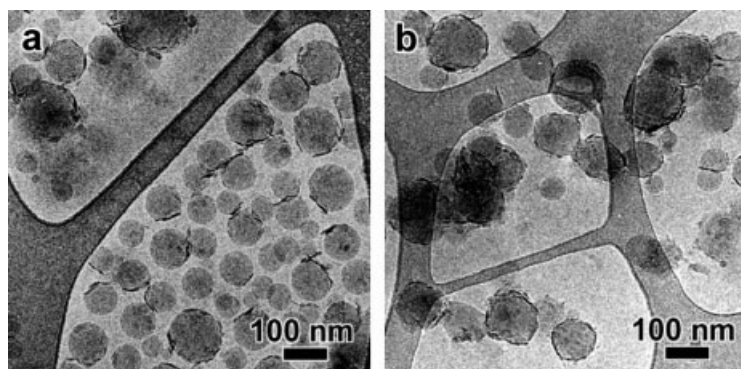
^b Determined by carbon elemental analysis of the supernatant solutions using Equation (4) and (5). Laponite = $10 \text{ g} \cdot \text{L}^{-1}$.

adsorbed amounts must be multiplied in this particular case by a factor of two. By doing so, it can be concluded that the amount of intercalated cations (either AIBA or MADQUAT) (e.g., 0.74 and $0.65 \text{ meq} \cdot \text{g}^{-1}$, respectively) are close to the CEC of laponite (i.e., $0.75 \text{ meq} \cdot \text{g}^{-1}$).

The preparation of stable organoclay suspensions in water is a prerequisite condition before performing the emulsion polymerization reaction. This requires extensive shaking for several days and the use of ultrasounds to help break down the clay agglomerates as shown in a recent paper from our group.^[12] However, emulsion polymerization reactions performed in these conditions yielded poorly stable latexes as the polymerization was taking place around clay aggregates.^[12] In an alternative strategy, we thus decided to perform a miniemulsion-like polymeriza-

tion reaction (see the “Experimental Part” for description of the procedure) where the organically-modified clay particles are sonicated together with the monomer. Under such conditions, the clay stability in water was greatly improved which allowed us to produce highly stable nanocomposite polymer latexes with high conversions.

Figure 6a and b show cryo-TEM images of composite particles prepared from the AIBA-laponite and MADQUAT-laponite intercalation complexes using this “mini-emulsion-like” polymerization recipe. In both cases, more or less spherical particles are observed with a diameter ranging from 30 to 130 nm. The spherical shape of the particles is more regular in the AIBA-laponite suspension while the nanoparticles are more aggregated in the MADQUAT-laponite sample. As seen from the distribution of dark “filaments,” the laponite

**Figure 6.**

Cryo-TEM images of polymer/laponite nanocomposite particles prepared using the “mini-emulsion-like” polymerization recipe in the presence of (a) AIBA-laponite and (b) MADQUAT-laponite.

platelets again form a shell around the polymer core. The larger (and darker) AIBA-laponite particles appear to have a rather homogeneous covering while only a small number of platelets are seen on the surface of the smaller nanospheres. The covering of the MADQUAT-laponite particles seems to be more heterogeneous which may also explain their more irregular shapes.

Conclusion

Silica/polystyrene and laponite/poly(sty-BA) nanocomposite latexes were synthesized through emulsion polymerization using different strategies.

To overcome the intrinsic hydrophilic character of the silica particles and to promote the growth of polymer on their surface, the surface was modified by grafting of alkoxy silane molecules or by adsorption of macromonomers. In the first route, we have shown that the morphology of the nanocomposite colloids can be finely tuned by varying the surface density of the reactive double bonds. Either flower-like or core-shell morphologies were obtained depending on the MPS grafting density. All the results reported in this article support the idea that the nucleation is taking place through the capture of the growing radicals by the silica particles. As the latter carry negative charges on their surface, they are able to stabilize the growing latex spheres whose number (and therefore overall surface area) is much larger than in the absence of silica. As the rate in emulsion polymerization is proportional to particles number, the kinetics of polymerization was strongly accelerated under these conditions. In the second route, double bonds on the silica surface are provided by the adsorption of the PEG macromonomer derivative. As the growing polymer nodules are simply physisorbed on the mineral surface, they are free to homogeneously organize onto silica giving rise to raspberry-like morphologies. The number of polymer nodules depends on the

silica to polymer particles size ratio and evolves as a function of time.

As far as clay minerals are concerned, we have shown that copolymer latexes, whose surface is decorated by functionalized laponite clay platelets, can be elaborated through emulsion polymerization. The clay powder was first modified by grafting of alkoxy silanes or by ion-exchange using either a cationic monomer (MADQUAT) or a cationic initiator (AIBA). Good clay dispersion into water (a key step of the present process) was achieved using a combination of an anionic surfactant and a peptizing agent. Stable latexes with low viscosities and full conversions were obtained in both cases suggesting a good incorporation of the clay platelets within the polymer suspension. Nanocomposite particles with “inverted” core-shell morphology (the clay platelets forming the shell of the particles) were successfully produced by this approach.

Acknowledgements: The authors thank Christian Novat and Nicolas Tissier (LCPP, Villeurbanne) for their great help in TEM analysis. E. Bourgeat-Lami and N. Negrete-Herrera thank the SFERE-CONACYT exchange program for its financial support. The gift of a sample of laponite RD by Rockwood Additives is also greatly acknowledged.

- [1] C. H. M. Hofman-Caris, *New J. Chem.* **1994**, 18, 1087.
- [2] A. D. Pomogalio, *Russ. Chem. Rev.* **2000**, 69, 53.
- [3] G. Kickelbick, *Prog. Polym. Sci.* **2002**, 28, 83.
- [4] V. Castelvetro, C. De Vita, *Adv. Coll. Interf. Sci.* **2004**, 108–109, 167.
- [5] E. Bourgeat-Lami, in: “*Encyclopedia of Nanoscience and Nanotechnology*”, H. S. Nalwa, Ed., American Scientific Publishers, Los Angeles **2004**, vol. 8, pp. 305–332.
- [6] E. Bourgeat-Lami, *J. Nanosci. Nanotechnol.* **2002**, 2, 1.
- [7] S. Reculosa, C. Mingotaud, E. Bourgeat-Lami, E. Duguet, S. Ravaine, *Nano Lett.* **2004**, 4, 1677.
- [8] E. Bourgeat-Lami, M. Insulaire, S. Reculosa, A. Perro, S. Ravaine, E. Duguet, *J. Nanosci. Nanotechnol.* **2005**, in press.
- [9] N. Negrete-Herrera, J.-M. Letoffe, J.-L. Putaux, L. David, E. Bourgeat-Lami, *Langmuir* **2004**, 20(5), 1564.
- [10] N. Negrete-Herrera, J.-M. Letoffe, J.-P. Reymond, E. Bourgeat-Lami, *J. Mater. Chem.* **2005**, 15, 863.

- [11] S. Reculosa, C. Poncet-Legrand, S. Ravaine, C. Mingotaud, E. Duguët, E. Bourgeat-Lami, *Chem. Mater.* **2002**, 14, 2354.
- [12] N. Negrete-Herrera, S. Persoz, J.-L. Putaux, L. David, E. Bourgeat-Lami, *J. Nanosci. Nanotechnol.* **2005**, in press.
- [13] N. Negrete-Herrera, J.-L. Putaux, E. Bourgeat-Lami, *Prog. Solid State Chem.* **2005**, in press.
- [14] S. Chalaye, E. Bourgeat-Lami, J.-L. Putaux, J. Lang, *Macromol. Symp.* **2001**, 169, 89.
- [15] M. Schappacher, A. Deffieux, J.-L. Putaux, P. Viville, R. Lazzaroni, *Macromolecules* **2003**, 36(15), 5776.
- [16] V. Durrieu, A. Gandini, M. N. Belcacem, A. Blayo, G. Eiselé, J.-L. Putaux, *J. Appl. Polym. Sci.* **2004**, 94(2), 700.
- [17] E. Bourgeat-Lami, P. Espiard, A. Guyot, *Polymer* **1995**, 36, 4385.
- [18] D. N. Furlong, J. R. Aston, *Colloids Surf.* **1982**, 4, 121.
- [19] W. Stöber, A. Fink, E. Bohn, *J. Colloid Interf. Sci.* **1968**, 26, 62.
- [20] S. Kang, S. I. Hong, C. R. Choe, M. Park, S. Rim, J. Kim, *Polymer* **2001**, 42, 879.
- [21] R. H. Ottewill, R. Satgurunathan, *Colloid Polym. Sci.* **1995**, 273, 379.
- [22] See for instance: [22a] M. Morvan, D. Espinat, J. Lambard, T. Zemb, *Colloids Surf. Pt. A* **1994**, 82, 193; [22b] B. S. Neumann, K. G. Sanson, *Israel J. Chem.* **1970**, 8, 315; [22c] J. D. F. Ramsay, S. W. Swanton, J. Bunce, *J. Chem. Soc. Faraday Trans.* **1990**, 86, 3919.
- [23] J.-M. Cases, *Chim. Phys.* **1969**, 66, 1602.
- [24] D. W. Thompson, J. T. Butterworth, *J. Colloid Interf. Sci.* **1992**, 151, 236.
- [25] A. Mourchid, E. Lécolier, H. van Damme, P. Levitz, *Langmuir* **1998**, 14, 4718.